EUROPEAN ORGANIZATION FOR NUCLEAR RESEARCH

ALICE-ANA-2016-xxx
June 17, 2016

Υ production at forward rapidity in $\mathbf{Pb-Pb}$ collisions at $\sqrt{s_{\mathrm{NN}}} = 5.02\,\mathbf{TeV}$

Lardeux Antoine[1], Das Indranil[2], Gaetano Fronze Gabriele[3,4]

1. CEA/IRFU, centre d'étude de Saclay, Gif-sur-Yvette
2. Saha Institute of Nuclear Physics, Kolkata
3. Universita e INFN, Torino 4. SUBATECH, Nantes

Email: antoine.lardeux@cern.ch, indranil.das@cern.ch, gabriele.gaetano.fronze@cern.ch
Twiki: https://twiki.cern.ch/twiki/bin/view/ALICE/UpsilonPbPb2015

Abstract

ALICE has measured the inclusive $\Upsilon(1S)$ and $\Upsilon(2S)$ production in $\mathrm{Pb-Pb}$ collisions at $\sqrt{s_{\mathrm{NN}}} = 5.02\,\mathrm{TeV}$. The measurement is performed at forward rapidity ($2.5 < y < 4$) and down to zero transverse momentum via the dimuon decay channel by analyzing the dimuon triggered events collected with the ALICE muon spectrometer apparatus. The nuclear modification factor (R_{AA}) of $\Upsilon(1S)$ has been computed as a function of the collision centrality and the $\Upsilon(1S)$ rapidity. The pp reference cross section used in this calculation has been determined by an extrapolation procedure based on various LHCb and ALICE results at different energies. An integrated $(0-90\%)$ $\Upsilon(1S)$ R_{AA} has been obtained for $2.5 < y < 4$ and $0 < p_{\mathrm{T}} < 12$ GeV/c such as:

$$R_{\mathrm{AA}}^{\Upsilon(1S)}(0-90\%) = 0.40 \pm 0.03\,(stat.) \pm 0.05\,(syst.)$$

Contents

1 Dataset, event and track selections

1.1 Data sample

Run The Υ analysis presented in this note is based on the first ALICE $\mathrm{Pb}-\mathrm{Pb}$ data taking of the LHC run 2 at a center of mass energy $\sqrt{s_{\mathrm{NN}}} = 5.02\,\mathrm{TeV}$ which took place in November-December 2015. A full description of the ALICE detectors can be found in [4]. The present study is performed on the AOD175, officially produced from the muon_calo_pass1 reconstruction of the LHC15o period including the latest alignement configuration, by analyzing the reconstructed tracks in the muon spectrometer apparatus. A detailed description of the muon reconstruction algorithm is given in [2,3]. A total of 137 runs pass the quality assurance checks (QA). The QA Muon report of this period can be found here.

Event selection The dataset analyzed is based on the dimuon events triggered by the muon spectormeter. More details can be found in [1,2]. A logical OR of CMUL7-B-NOPF-MUFAST (unlike sign dimuon low p_{T} threshold) and CMLL7-B-NOPF-MUFAST (like sign dimuon low p_{T} threshold) trigger classes is used to filter the dimuon events. The like sign dimuons are selected in order to perform the event mixing procedure (normalization method 5.1) as well as the CMSL-B-NOPF-MUFAST (single muon low p_{T} threshold). In order to reject the beam-gas and debunched collisions the physics selection cuts are applied. The remaining dataset is then filtered to select events which are within the centrality class of $0-90\%$. More details on the centrality estimation can be found here.

1.2 Track and pair selection

In order to clean the dataset of tracks with the aim of forming the opposite sign dimuon invariant mass spectrum we require that the following conditions are satisfied for each tracks and pairs:

track cuts

- $-4.0 < \eta < -2.5$ to reject tracks at the edges of the spectrometer acceptance,
- $17.6 < R_{\mathrm{abs}} < 89.5$ to remove tracks crossing the thicker part of the front absorber,
- matching between a reconstructed trigger track passing the hardware Low p_{T} threshold ($p_{\mathrm{T}}^{\mathrm{trig}} > 1$ GeV/c) and a reconstructed tracker track,
- pDCA: product of the track momentum p by the distance of the extrapolated track to the transverse plane containing the vertex DCA (Distance of Closest Approach). This selection remove the fake tracks (tracks which do not point to the vertex) present essentially in central collisions. A cut has been tuned on data and set to $6 \times \sigma_{p\mathrm{DCA}}$, where $\sigma_{p\mathrm{DCA}}$ is the resolution of this quantity.
- $p_{\mathrm{T}} > 2$ GeV/c: this selection reduces significantly the combinatorial background by increasing the significance of the signal. A study has been performed on the embedding MC production. The distributions of the opposite sign dimuon identified as background (left) and as Υ(1S) embedded signal (right), after applying all the previous track cuts including pDCA, are represented on the figure 1 as a function of the p_{T} of each muon according to their sign. A cut at 2 GeV/c has been chosen as in previous Υ analyses. The evolution of the significance as a function of the p_{T} cut applied on each muons can be observed on the figure 2. The maximum of significance is find for $p_{\mathrm{T}}^{\mu^+} = p_{\mathrm{T}}^{\mu^-} = 2.5$ GeV/c. Nevertheless, the increase of significance in raw data by applying a muon p_{T} cut of 2.5 GeV/c with respect 2 GeV/c is negligible. Furthermore, a muon p_{T} cut at 2 GeV/c remove almost no Υ(1S) signal ($< 1\%$). Thus none systematic uncertainty has been assigned to this track cut.

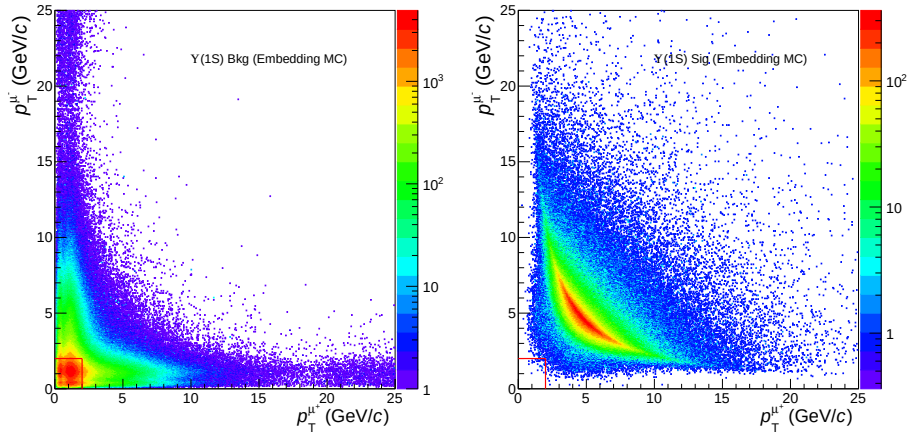

Fig. 1: Background (left) and Υ(1S) signal (right) distributions as a function of the p_{T} of each muon extracted from embedding MC.

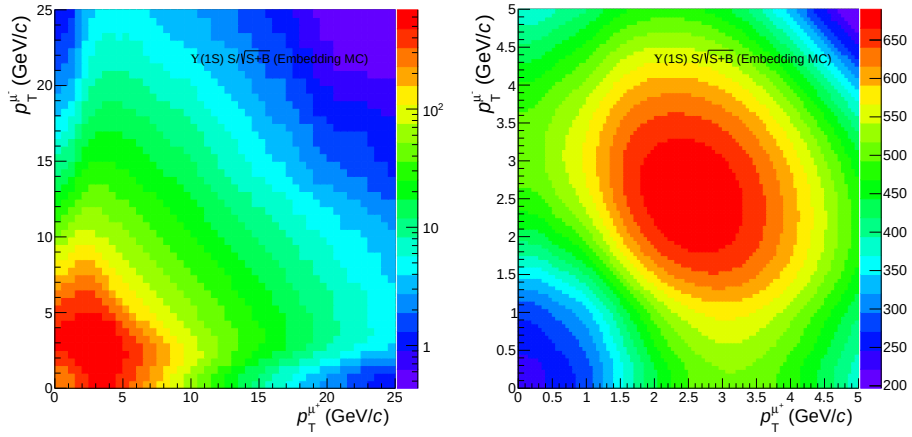

Fig. 2: Υ(1S) significance as a function of the p_{T} cut of each muon computed from embedding MC.

Pair cuts

- opposite charge
- $-4 < y < -2.5$
- $p_{\mathrm{T}} < 12$

2 Signal extraction

The signal extraction of bottomonium resonances have been performed through a fit of the invariant mass spectrum of opposite sign tracks reconstructed within the muon spectrometer (after applying the track and pair cuts mentioned in section 1.2). The spectrum is composed of two sources: a continuum and the Υ signals above. The signal shape is parametrized by an extended Crystal-Ball (CB2) with its tails tuned on MC (cf 5.1) and the background one by an ad-hoc function such as a sum of two exponential. The same function is used for the three Υ resonances. The mass position and the width of the $\Upsilon(1S)$ are left free. The mass position of higher states are scaled to the one of the $\Upsilon(1S)$ according to the PDG mass ratios and their widths to the ratios obtained in MC such as:

$$m_{\Upsilon(2S)} = m_{\Upsilon(1S)} \cdot \frac{m^{\mathrm{PDG}}_{\Upsilon(2S)}}{m^{\mathrm{PDG}}_{\Upsilon(1S)}},$$

$$\sigma_{\Upsilon(2S)} = \sigma_{\Upsilon(1S)} \cdot \frac{\sigma^{\mathrm{MC}}_{\Upsilon(2S)}}{\sigma^{\mathrm{MC}}_{\Upsilon(1S)}}.$$

Thanks to the luminosity collected we are able to split the centrality dependence in 4 classes (0-10%, 10-30%, 30-50%, 5090%) and the rapidity dependence in 3 intervals. Fits results can be appreciate as a function of centrality on figure 3 and as a function of rapidity on figure 4. A total amount of ≈ 1100 $\Upsilon(1S)$ have been measured. The significance is ranging between 6 and 13 and the statistical uncertainty between 4 and 14%.

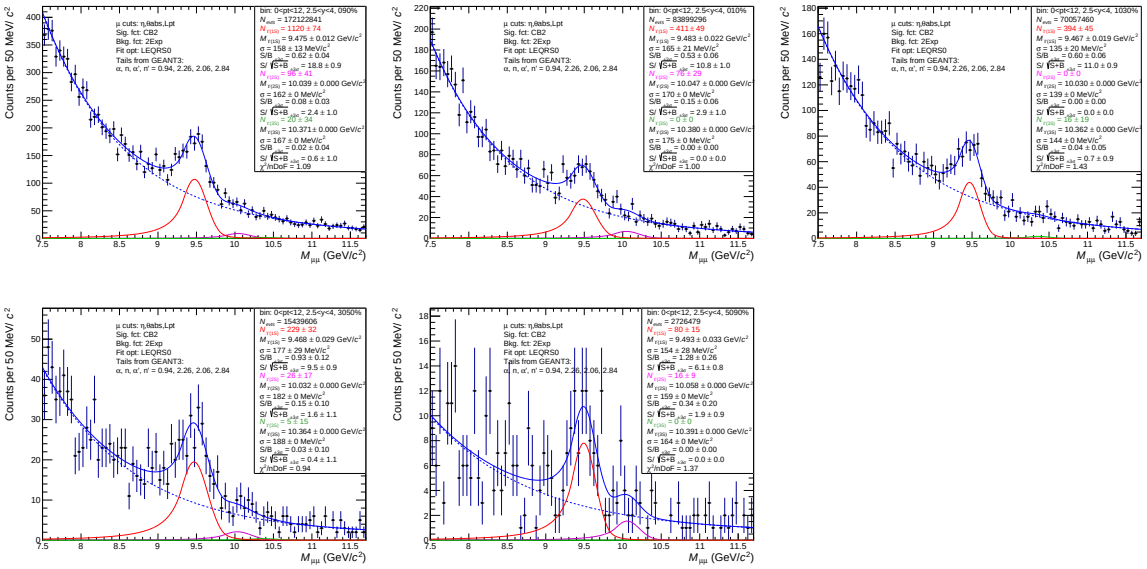

Fig. 3: Signal extraction in centrality classes

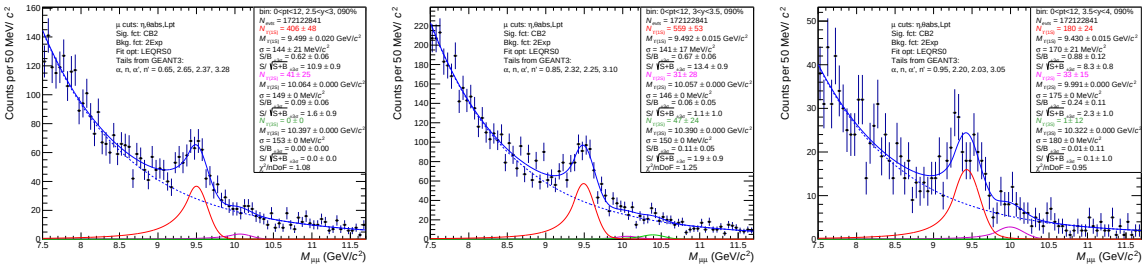

Fig. 4: Signal extraction in rapidity bins

3 Nuclear modification factor

The Υ(1S) nuclear modification factor ($R_{\rm AA}$) is computed such as:

$$R^i_{\rm AA} = \frac{{\rm d}^2 N^{\rm measured,\,i}_{\Upsilon({\rm 1S})}/{\rm d}p_{\rm T}{\rm d}y}{\langle T^i_{\rm AA}\rangle\, BR_{\Upsilon({\rm 1S})\to\mu^+\mu^-}\, A\epsilon^i\, N^{{\rm MB},\,i}_{evt}\, {\rm d}^2\sigma^{\rm pp}_{\Upsilon({\rm 1S})}/{\rm d}p_{\rm T}{\rm d}y}.$$

where:

- $N^{\rm measured,\,i}$ is the number of Υ(1S) measured in the centrality bin i (cf 3),
- $\langle T^i_{\rm AA}\rangle$ is the nuclear overlap function (values),
- $BR_{\Upsilon({\rm 1S})\to\mu^+\mu^-}$ is the branching ratio of Υ(1S) decaying in two muons (2.48%),
- $A\epsilon^i$ is the acceptance times efficiency correction of the muon spectrometer (cf 2),
- $N^{{\rm MB},\,i}_{evt}$ represent the equivalent number of Minimum Bias events with respect to the number of dimuon triggered events (CMUL) by taking into account its dead time (cf 3),
- $\sigma^{\rm pp}_{\Upsilon({\rm 1S})}$ is the Υ(1S) pp cross section at $\sqrt{s} = [5.02{\rm TeV}]$.

$N^{\rm MB}$ The equivalent number of MB events is obtained run by run via the determination of the normalization factor ($F_{\rm norm}$) describes in the charmonium analysis note of the same data taking period and available here. The mean value of the normalization factor over the full period is equal to $11.84 \pm 0.01(stat.)$ for the centrality class 0-90%. Finally a total number of $1.5.10^9$ MB events within 0-90% centrality class is analyzed.

$\sigma^{\rm pp}_{\Upsilon({\rm 1S})}$ The Υ(1S) pp reference has been estimated by extrapolation from different models and from LHCb and ALICE measurements at lower and higher energies. A common public note has been published (CDS). The values reported in table 1 have been computed for the rapidity region cover by the muon spectrometer ($-4 < y < -2.5$) and three rapidity points which correspond to 2.75, 3.25 and 3.75.

y	$\sigma^{\rm pp}_{\Upsilon({\rm 1S})}$ (nb)
$[2.5-4]$	1.14 ± 0.10 (8.8%)
$[2.5-3]$	0.484 ± 0.038 (7.9%)
$[3-3.5]$	0.376 ± 0.045 (12.0%)
$[3.5-4]$	0.257 ± 0.029 (11.3%)

Table 1: Υ(1S) pp cross section at $\sqrt{s} = [5.02{\rm TeV}]$ computed by extrapolation.

$A\epsilon$ The spectrometer correction of acceptance times efficiency is computed in the embedding MC (production LHC16e2 & plus), thus we are able to reproduce the realistic occupancy of the muon tracking chambers as a function of the collision centrality. A total of 1 937 708 Υ(1S) has been embedded in CINT7-B-NOPF-MUFAST events. Two scaling have to be achieved in order to get the proper $A\epsilon$ correction:

- as a function of the number of CMUL events analyzed per run to account for the time evolution of the apparatus and the relative statistic available,
- as a function of the collision centrality by using the mean number of binary collisions because the centrality distribution of CINT7 events is flat unlike the CMUL7 events.

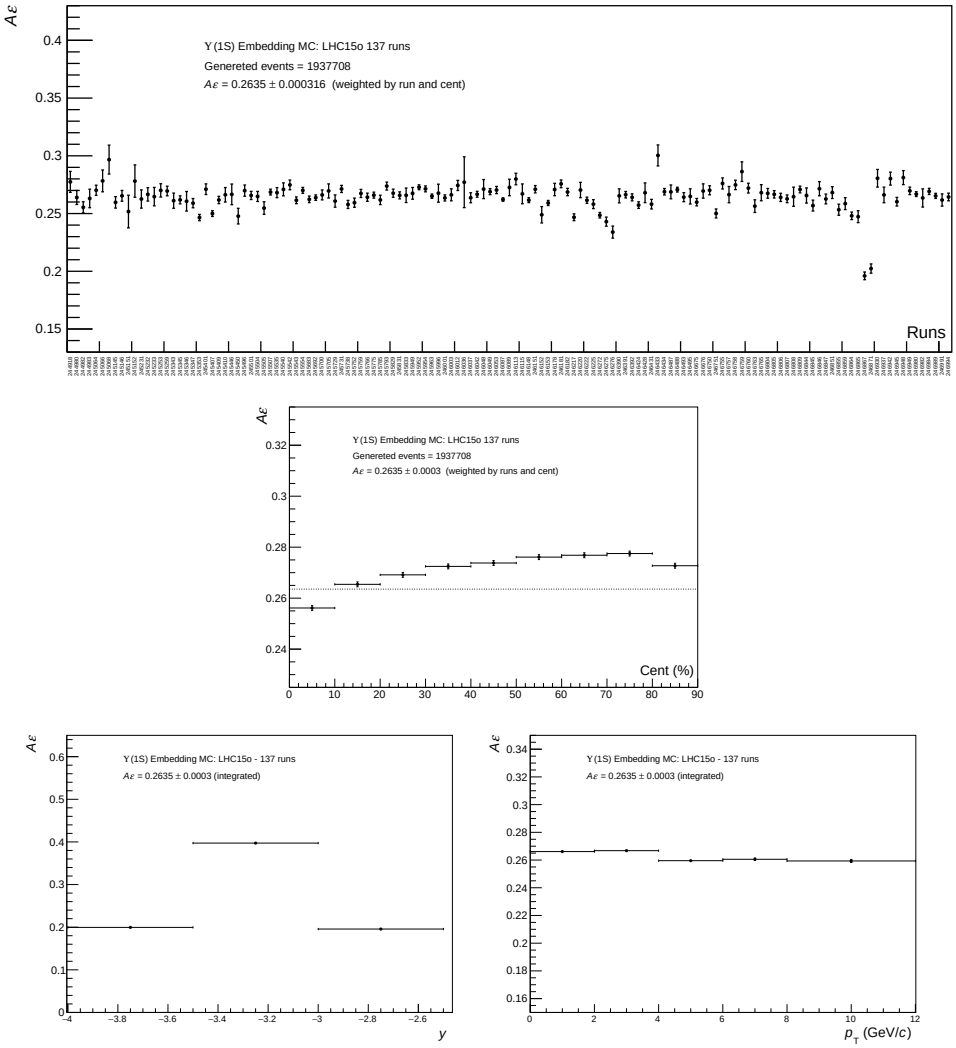

Fig. 5: $A\epsilon$ correction extracted from embedding MC as a function of the run number (top), the collision centrality (center), the Υ(1S) rapidity (bottom left) and the Υ(1S) transverse momentum (bottom right).

The $A\epsilon$ results are shown as a function of the run number, the collision centrality, the Υ(1S) y and p_{T} on figure 5. We can observe a good stability of the muon spectrometer capabilities in time. A drop of around 8% of the $A\epsilon$ is observe going from peripheral to central collisions as expected and already seen in previous data. Finally an integrated Υ(1S) correction of $26.35 \pm 0.03(stat.)$% has been found. The centrality and rapidity dependence results are reported in the table 2.

centrality	$A\epsilon \pm (stat.)$ (%)	y	$A\epsilon \pm (stat.)$ (%)
0-10%	25.61 ± 0.09	$[2.5-3]$	19.56 ± 0.04
10-30%	26.68 ± 0.07	$[3-3.5]$	39.73 ± 0.06
30-50%	27.29 ± 0.07	$[3.5-4]$	19.95 ± 0.029
50-90%	27.63 ± 0.05		
0-20%	25.97 ± 0.07		
20-90%	27.15 ± 0.04		

Table 2: Υ(1S) $A\epsilon$ correction values for the centrality and rapidity intervals under study and obtained from embedding MC. The statistical uncertainties quoted here and related to the deep of the MC sample are negligible.

5 Systematics

In the following we list and discuss the different sources of uncertainties entering into account in the $R_{\rm AA}$computation. The main sources are those on the pp reference and the signal extraction. A summary table is provided at the end of the section (7).

5.1 Signal extraction systematic

Several tests are performed to estimate the systematic uncertainty related to the signal and background shapes as well as the fixed parameters like the Υ(2S) width. The different tests are presented thereafter.

Set of tails Since the CB2 function reproduces well the signal (>99%), only the sets of tails fixed on MC are tested. For that we have extracted, via the same fit procedure as in data, the tail parameters from the invariant mass of reconstructed Υ(1S) signal generated in MC simulations. A pure Υ(1S) MC sample has been produced with Geant4 transport codes to be compared to the embedding MC sample based on Geant3 transport code. The sets of tails extracted from the integrated spectra are shown on figure 7 Due to the small statistics of signal in raw data and the quite high resolution of the pic the effect of the tails on the amount of measured Υ(1S) is small. Integrated over $p_{\rm T}$ and y intervals the difference is less than 1% level, reaching a maximum of 3% as a function of y. Note that an other set of tails extracted in pp data at $\sqrt{s} = 13$ TeV for which the SB ratio and integrated luminosity is much higher has been tested. Nevertheless the parameters being not enough constrained the results return by the fit was unrealistic. That was the same by letting the tails free. The centrality and rapidity dependence of the tail parameters has been study in embedding MC sample. The results are reported on the figure 8. We observed a significant variation as a function of y and a small evolution of the right tail as a function of centrality which is not significative. Finally two sets of tails are used i(pure Υ(1S) MC with G4 and embedding MC with G3) in the evaluation of the signal extraction systematic. Their rapidity dependence is taken into account and the set extracted from the integrated centrality classes (0-90%) is used for all centrality classes.

Υ(2S) and Υ(3S) widths Due to the poor S/B ratio of higher resonances one have to fix their width. As explained in section 2, the widths are scaled to the Υ(1S) width, left it free, by the ratio obtained in MC. In both MC samples these ratio are very close and $\sigma_{\Upsilon(2S)}/\sigma_{\Upsilon(1S)} = 1.03$ and $\sigma_{\Upsilon(3S)}/\sigma_{\Upsilon(1S)} = 1.06$. To test the validity of this scaling one vary the higher resonance widths by the relative uncertainty of the Υ(1S) width parameter return by the fit in data. Note that

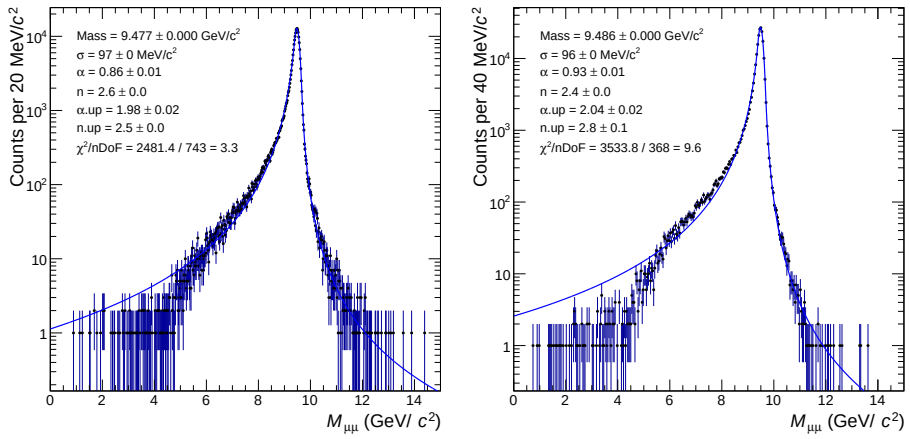

Fig. 7: Fit of the signal shapes obtained in embedding (left) and pure (right) Υ(1S) MC samples with a CB2 function.

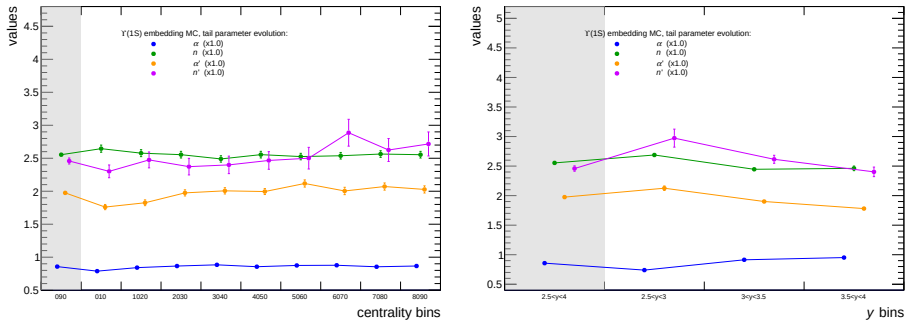

Fig. 8: Centrality (left) and rapidity evolution of the tail parameters. The grey bands correspond to the integrated result.

it has been testing to let the Υ(2S) and Υ(3S) width free in data, unfortunately the signal is too small to constrain significantly the width parameter giving an uncertainty beyond 100%. A maximum uncertainty of 10% is observed for the Υ(1S) and used to perform two tests in $\pm 1\sigma$ of the scaled Υ(2S) and Υ(3S) widths in the same direction for both. Since the Υ(2S) and Υ(3S) signals do not affect the Υ(1S) one as a fonction of centrality and rapidity these two tests are performed only for the integrated invariant mass spectrum.

Background function To test the background reproduction several ad hoc functions are used. As in previous Υ analyses, a sum of two exponential and a sum of two power law are used. Both functions return a good χ^2 never exceeding 1.8. The observed variation goes up to 10% for the integrated spectrum.

Fitting range To check the stability of the fitting procedure an additional test by varying the fitting range of the dimuon invariant mass spectrum is Thus different ranges have been tried (narrow, wide, etc). The results reported in this note are obtained by operating two fitting ranges: $6 < m_{\mu\mu} < 13$ GeV/c and $7 < m_{\mu\mu} < 14$ GeV/c. The observed variation goes up to 7% for the integrated spectrum.

Event mixing Finally, in order to improve the reproduction of the background shape the event mixing technic has been performed. From our past experience, it has been demonstrated that the single muon low p_{T} threshold (CMSL7) dataset is the best one to reproduce the like sign muon pairs invariant mass distribution obtained by analyzing the CMUL7 or CMLL7 triggered events. 9 pools of events are formed according to their centrality (interval of 10%) in order to mix similar events in term of multiplicity for instance. That procedure is a run by run basis to account for the time evolution of the apparatus. It has been checked that the merging of the mixed spectra over the run numbers has a negligible effect whether it is made before or after normalization. It is therefore realized before. Furthermore, it has also been checked that the best normalization method is the one based on the like sign muon pairs distributions such as, unlike the integral method of the :

$$\int_5^{14} N_{mix}^{+-}\, dM = \int_5^{14} 2R\sqrt{N_{raw}^{++} N_{raw}^{--}}\, dM$$

$$\text{with} \quad R = \frac{N_{mix}^{+-}}{2\sqrt{N_{mix}^{++} N_{mix}^{--}}},$$

which accounts for the difference acceptances between μ^+ and μ^-. Due to the high momentum carried out by the muon entering in the high mass region off the invariant mass, the R factor is flat and equal to 1 as a function of the dimuon invariant mass. Thus the determination of the normalization factor can be achieved on the full mass range of the fit including the upsilon mass

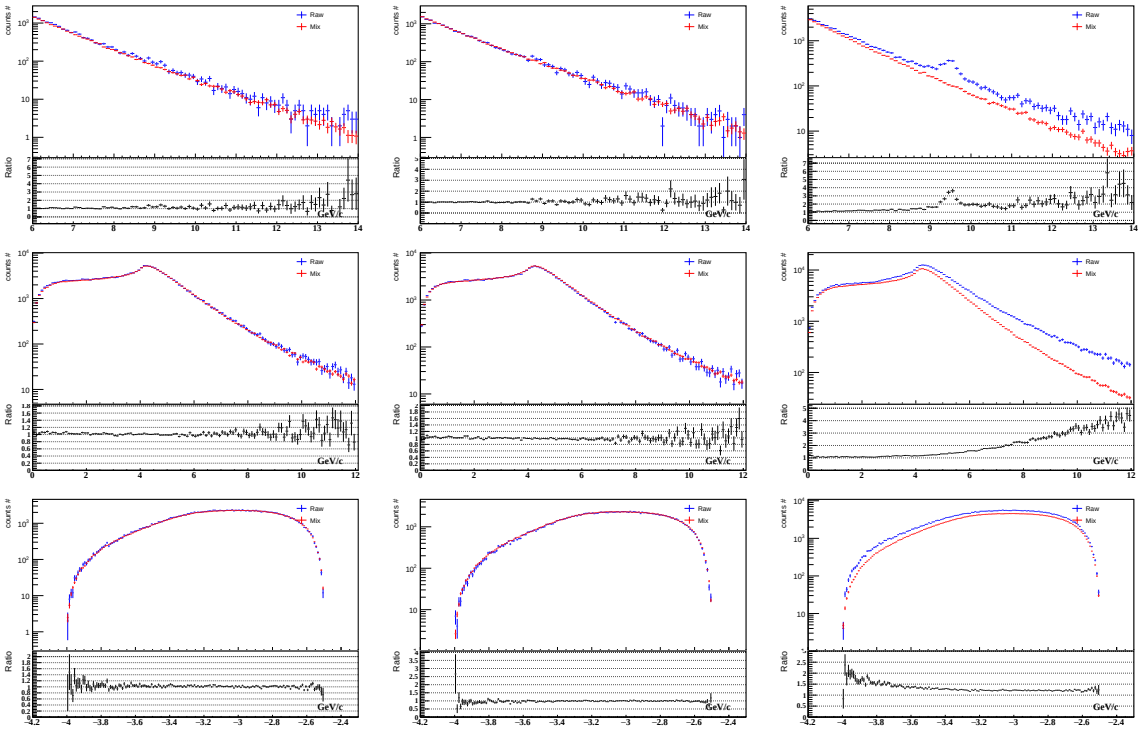

Fig. 9: Comparison of raw and normalized mixed spectra as a function of invariant mass (top), p_{T} (center) and y (bottom) for positive like sign dimuon (left), negative like sign dimuon (center) and unlike sign dimuon (right).

region. Note that due to the decreasing trend of the CMSL7 event distribution as a function of centrality, the normalisation procedure should be apply per centrality pool before any merging of centrality classes. The resulting normalized mixed spectra are compared on figure 9 to the the raw ones as a function of the invariance mass (first raw), the dimuon p_{T} (second raw) and y (third raw) for positive like sign dimuon (first column), negative like sign dimuon (second column) and the opposite sign dimuon (third column). We can appreciate the good reproduction of the background by looking the flat ratios obtained between like sign dimuon distributions. Finally the normalized mixed spectrum is subtracted to the raw one. The resulting subtracted invariant mass distributions are then used as alternative input distributions for estimating the signal extraction systematic uncertainty. All the tests described above are applied for which only the ad hoc background functions change to either one exponential or one power law.

To conclude, 48 tests are performed for the integrated spectrum whereas 16 tests are performed for all other spectra. The mean value over all the tests is taken as the number of extracted Υ(1S) as well as the mean value of the statistical uncertainties return by the fits on the integral of the signal function between 0 to 15 GeV/c^2. The systematic uncertainty on the signal extraction is defined by the RMS of the distribution of tests shown in the figure 10. It has

centrality	$N^{\Upsilon(1S)}$	y	$N^{\Upsilon(1S)}$
0-10%	$393 \pm 41\ (10.4\%) \pm 22\ (5.6\%)$	$[2.5-4]$	$1107 \pm 70\ (6.3\%) \pm 43\ (3.9\%)$
10-30%	$407 \pm 41\ (10.1\%) \pm 21\ (5.1\%)$	$[2.5-3]$	$398 \pm 43\ (10.8\%) \pm 17\ (4.2\%)$
30-50%	$218 \pm 34\ (15.6\%) \pm 10\ (4.4\%)$	$[3-3.5]$	$548 \pm 48\ (8.8\%) \pm 30\ (5.4\%)$
50-90%	$75 \pm 15\ (20.0\%) \pm 3\ (4.5\%)$	$[3.5-4]$	$167 \pm 23\ (13.7\%) \pm 11\ (6.9\%)$
0-20%	$603 \pm 50\ (8.3\%) \pm 29\ (4.9\%)$		
20-90%	$506 \pm 46\ (9.2\%) \pm 27\ (5.4\%)$		

Table 3: Υ(1S) raw yield as a function of centrality classes and rapidity.

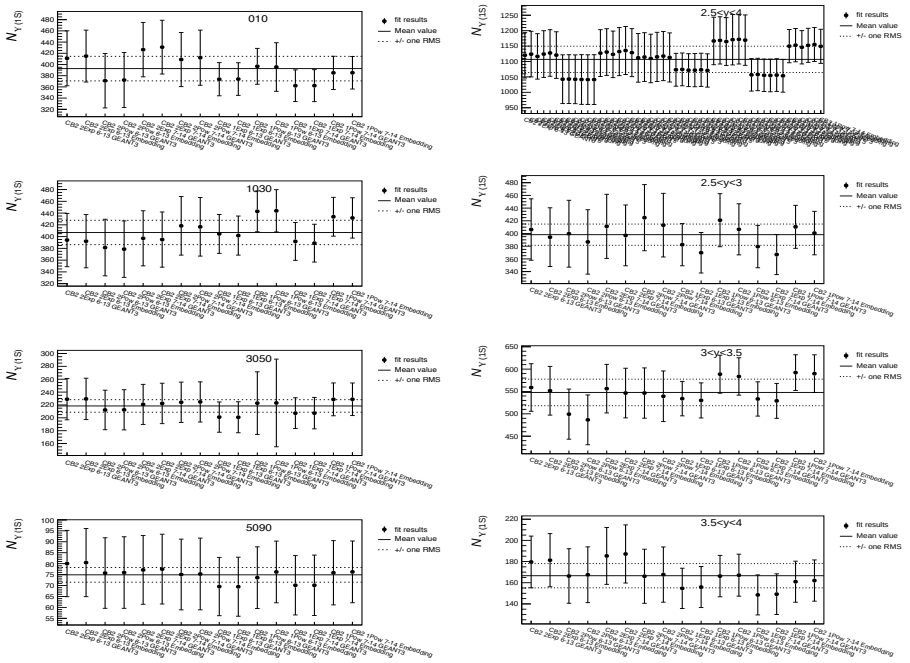

Fig. 10: Number of measured ϒ(1S) as a function of the different tests for the centrality classes (left) and integrated spectrum and rapidity intervals (right).

been checked that all the tests for all the intervals under study do not exceed 2 RMS. All the results are reported in the table 3. The systematic uncertainty varies between 4% (integrated spectrum) to 7% (most forward interval).

5.2 MC systematic

The MC productions like pure simulation or embedding are based on input p_{T} and y distributions. The parametrization used for both productions is defined as the product of the pp parametrization available in AliGenMuonLib class at 5 TeV times a shadowing parametrization at 2.76 TeV similar to EKS98. In order to test the validity of this parameterization and determine a associated systematic uncertainty we have computed the ϒ(1S) $A\epsilon$ correction from various kinematic shapes represented on the figure 11 such as: PbPb at 14 TeV, PbPb at 4 TeV extrapolated from CDF data, PbPb at 2.76 TeV and also a pp parameterization at 5 TeV. Note

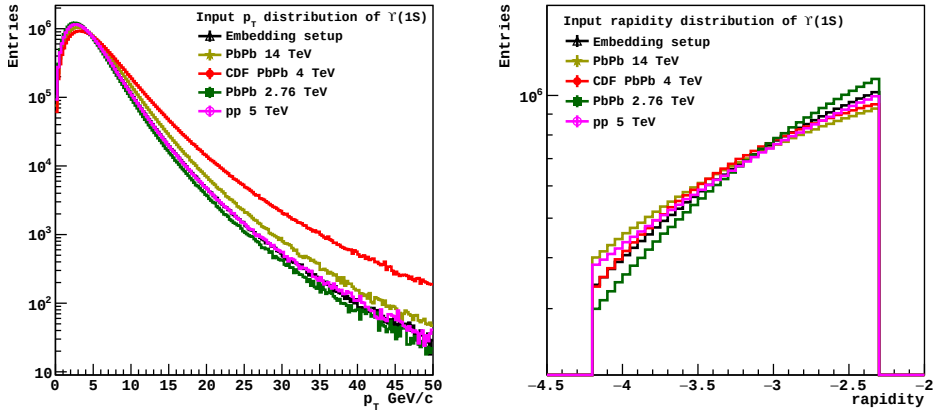

Fig. 11: Input p_{T} and y distributions for different simultion setups.

that due to the small statistic available we can not apply a iterative data-driven method as in the J/ψ case. The $A\epsilon$ results are shown as a function of the run number, $p_{\rm T}$ and y on the figure 12. The maximum relative difference between the various input parametrization is taken as input MC systematic uncertainty and is $\sim 1\%$ in the integrated case, almost flat and $\sim 2\%$ as a function of $p_{\rm T}$ and a variation of 1-3% is observed as a function of y. The input MC systematic is correlated as a function of centrality and not as a function of $p_{\rm T}$ and y. TBCompleted

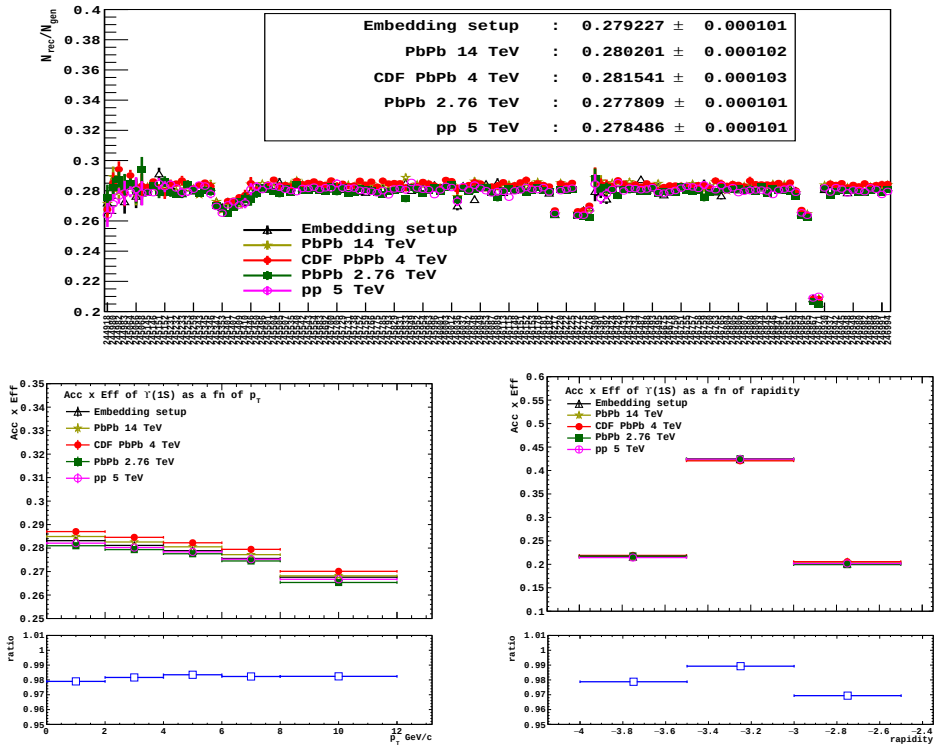

Fig. 12: $A\epsilon$ as function of run numbers integrated over $p_{\rm T}$ and y for different input parameterizations. The maximum relative difference of $100 \times (1 - \frac{0.2778}{0.2815}) = 1.3\% \sim 1\%$ is taken as MC systematics on integrated results. (Results in earlier analysis on Υ suppression in 2.76 TeV found 4%) In $p_{\rm T}$ and y bins a variation of 1-3% have been found.

5.3 Tracker systematic

The determination of the tracking efficiency of the muon spectrometer and its systematic uncertainties are reported in details in the section 7 of the J/ψ analysis note (here) referring to the same Pb-Pb data sample (LHC15o period). A 1.5% systematics uncertainty is observed in average for single muons, with variations depending on the kinematics, the maximum being always with $2-3\sigma$. This results in a 3% systematics uncertainty for dimuons, considered as fully correlated as a function of centrality but not as a function of $p_{\rm T}$ and y. Another source of uncertainty comes from the loss of tracking efficiency with increasing collision centrality, as the detector occupancy increases. This loss of efficiency is reproduced by embedding simulated Υ(1S) into real events as it could be observed on the figure 5. The differences in the efficiency drop between data and MC amount to $\sim 0.5\%$ in most central collisions, which results in a systematic uncertainty of $\sim 1\%$ for J/ψ which should be even lower for Υ(1S). This uncertainty decreases with decreasing centrality, down to 0 in peripheral events, and is considered as fully correlated as a function of $p_{\rm T}$ and y.

5.4 Trigger systematics

Three different sources of systematic uncertainties have been taken into account with respect to the muon trigger system:

- the real trigger response is different with respect to the one used in Montecarlo simulations;
- the efficiency values measured using real data are used as part of the Montecarlo input. Different methods can be used to evaluate the efficiency. Each method provides a slightly different efficiency value that has to be evaluated;
- the $A \times \epsilon$ used within simulations can be altered by the efficiency evaluation method, as discussed in the previous point. The variation of $A \times \epsilon$ should be evaluated as well.

Each of these points should be considered in order to provide a comprehensive quotation of the overall systematic uncertainty.

5.4.1 Trigger response

The trigger response is defined as in equation 1, where:

- Lpt: Low p_t, $p_t > 0.5$ GeV/c cut;
- Apt: All p_t, no p_t cut

$$RF_{(MC,Data)} = \frac{N_{Lpt_{(MC,Data)}}}{N_{Apt_{(MC,Data)}}} \tag{1}$$

The RF_{Data} has been obtained using the full Pb-Pb $\sqrt{S_{NN}} = 5.02TeV$ data sample, while the RF_{MC} has been computed analyzing a simulated data sample $10\times$ greater, in order to limit statistical uncertainties. The RF should be studied with respect to p_t and pseudo-rapidity (η). When studied with respect to p_t the RF grows asymptotically to the unity by contruction.

Rescaling procedure The RF expresses the ratio between the number of Lpt and Apt matches. The corrected number of Lpt_{MC} matches can be obtained as expressed in equation 2.

$$N_{\text{corrected } Lpt_{MC} \text{ with } RF_{(MC,Data)}} = N_{Apt_{MC}} \cdot RF_{(MC,Data)} \tag{2}$$

The application of the quoted correction allows to correct the invariant mass spectra in order to evaluate the variation induced by the difference between the real and the simulated RFs. Each entry of an invariant mass spectrum is the invariant mass of a dimuon pair. Usually the dimuon invariant mass spectrum is obtained requiring the track to match Lpt condition. The corrected spectrum is obtained by requiring on the single tracks to match Apt and then by assigning a weight to every track pair in order to rescale the number of Apt matches to the Lpt.

Operational choices In order to obtain a precise result the RF can be evaluated with different levels of granularity. Instead of obtaining one $RF(p_t)$ integrated in rapidity we have divided the rapidity range in 10 sub-ranges. In such a way the $RF(p_t)$ becomes $RF(p_t;\eta)$. The RF can be treated in two different ways, which converge in case of high statistics:

- the RF is a functional form obtained via fitting the $\frac{Lpt}{Apt}$ histogram. This method can interpolate points in order to solve holes in the distribution, but has the drawback that the analytic form of the RF is not defined *a priori*;

– the $\frac{Lpt}{Apt}$ histogram per bin content can be directly used as the required weight, avoiding the fitting procedures and related NLO uncertainties. This method can't anyway be used in case of low statistics, since in that case fluctuations and holes risk to provide wrong weights to some of the entries.

Both approaches have been pursued. The results are compatible within uncertainties, hence the direct use of histograms has been chosen as the adopted approach.

Entries weighting procedure Each track pair composed of track which passed the Apt selection has to be used to fill the invariant mass spectrum. The analysis cut is Lpt, so the number of Lpt pairs should be obtained starting from the Apt pairs. The previously computed ratio between Lpt and Apt matches allows to do so by assigning a weight to each track pair. The weight is the product of the two RFs values obtained for each of the two paired tracks, as expressed in 3, where p_{t1} and η_1 are the values of the first track composing the pair and p_{t2} and η_2 are the values of the second.

$$weight_{(MC,Data)}(p_{t1},p_{t2};\eta_1,\eta_{t2}) = RF_{(MC,Data)}(p_{t1};\eta_1)\cdot RF_{(MC,Data)}(p_{t2};\eta_2) \tag{3}$$

Systematic uncertainty evaluation In order to cope with the analysis choices the spectrometer rapidity acceptance range (2.5<y<4.0) has been divided in three rapidity region. One invariant mass spectrum has been computed for each region. The rapidity binning refers to the dimuon rapidity. The weighting procedure has been applied using both MC and Data weights, obtaining two invariant mass spectra for each dimuon rapidity bin, hence for each rapidity bin two invariant mass spectra have been computed. The systematic uncertainty has been evaluated as the relative difference of the integral of the two spectra, as reported in 4, where f_{MC} and f_{Data} are the invariant mass spectra corrected using respectively $weight_{(MC)}$ and $weight_{(Data)}$.

$$Syst_{RF} = \frac{|\int f_{MC}(m)dm - \int f_{Data}(m)dm|}{\int f_{Data}(m)dm} \tag{4}$$

Results In table 6 the computed values for systematic uncertainties related to the response function are reported as percent values in the studied rapidity bins.

η interval	$Syst_{RF}(\%)$
$2.5 < \eta < 3.0$	0.1%
$3.0 < \eta < 3.5$	0.1%
$3.5 < \eta < 4.0$	0.1%

Table 4: Systematic uncertainties induced by the difference between response functions.

5.4.2 Efficiency systematic error

The efficiency of the muon trigger is evaluated using one of multiple possible methods. The efficiency measured during data taking is stored in a OCDB file available on AliEn. The choice of one of the possible efficiency evaluation methods can introduce a wrong estimation of the efficiency. In order to take into account the contribution of this possible bias is necessary to perform the efficiency evaluation using different methods. From the various efficiency values a spreading value is computed.

All the Montecarlo simulations performed use the OCDB measured during real data taking, which contains the standard efficiencies. A custom OCDB must be created in order to inject the spreading measured as presented above. In particular the spreading is subtracted from the standard efficiency in order to simulate the worst case scenario.

At this point two Montecarlo simulations should be performed: the first one should use the efficiency values contained in the standard OCDB file, while the second one has to retrieve the efficiencies from the customized OCDB. The invariant mass spectra obtained from the analysis of the two Montecarlo productions have been cut in different rapidity bins and integrated over p_t and m_{inv}. The aim of this procedure is to evaluate the systematic uncertainty on the signal values, hence only tracks which Montecarlo truth corresponds to muons from upsilon are considered while filling the spectrum. The reported systematic uncertainty derived from the method adopted for the efficiency evaluation has been computed using the equation reported 5, where the scaling trough the number of analyzed events is necessary to take in account the possible differences between the two Montecarlo productions. Results for the systematic's evaluation are reported in table 5.

$$Syst_{Eff}(\eta) = N_{(stdOCDBevents)} \cdot \frac{|\frac{\int f_{MC;\eta}(m)dm}{N_{(modOCDBevents)}} - \frac{\int f_{Data;\eta}(m)dm}{N_{(stdOCDBevents)}}|}{\int f_{Data;\eta}(m)dm} \tag{5}$$

η interval	Standard OCDB events	Custom OCDB events	$Syst_{Eff}(\%)$
$2.5 < \eta < 3.0$	44523	42936	1.82%
$3.0 < \eta < 3.5$	71832	69526	1.45%
$3.5 < \eta < 4.0$	27012	26314	0.80%
Total N_{events}	632389	620969	

Table 5: Systematic uncertainties induced by the uncertainty on efficiency values.

5.4.3 $A \times \epsilon$ systematic error

The efficiency systematic error due to the choice of the efficiency evaluation method modifies the A values. The method presented in section 5.4.2 is adopted in this part of the evaluation of systematics with some variations. The same two Montecarlo simulations performed for the first systematic evaluation have been analyzed using another approach in order to measure the contribution of the third source of systematic uncertainties. The A is defined as reported in equation 6, where the dependencies of the computed value are arbitrary based on the analysis choices.

$$A \times \epsilon(p_t, y) = \frac{N_{\text{reconstructed muons}}(p_t, y)}{N_{\text{simulated muons}}(p_t, y)} \tag{6}$$

The procedure asks to perform two steps analysis in order to retain all the data needed to compute the studied parameter:

- collect the reconstructed muon pairs which came from a upsilon;
- collect the generated muon pairs from a upsilon.

The muons reconstructed data and Montecarlo truth are then stored in the chosen histograms keeping the needed dependencies. In this work the tracks have been divided in three rapidity bins to cope with the analysis choices previously presented. The A can then be computed using the equation 6 applied bin by bin on the stored histograms. This procedure should be applied to both the Montecarlo simulations, namely the first performed using the standard OCDB, the second with the customized OCDB, which contains the dropped efficiencies. At this point two A trends for each rapidity bin are available. The systematic uncertainty induced by the efficiency uncertainty on the A is then evaluated as reported in equation 7.

$$Syst_{A\times\epsilon}(y) = \frac{|\int A\times\epsilon_{stdOCDB}(p_t,y)dp_t - \int A\times\epsilon_{modOCDB}(p_t,y)dp_t|}{\int A\times\epsilon_{stdOCDB}(p_t,y)dp_t} \quad (7)$$

The computed values are reported in table 6.

η interval	$Syst_{A\times\epsilon}(\%)$
$2.5 < \eta < 3.0$	1.78%
$3.0 < \eta < 3.5$	1.60%
$3.5 < \eta < 4.0$	0.45%

Table 6: Systematic uncertainties induced by the difference between response functions.

5.5 Centrality determination systematic

TBW

5.6 Other systematics

As it has been presented in Section 3, other ingredients enter in the computation of the Υ(1S) nuclear modification factor. The nuclear overlap function is determine through the ALICE centrality framework discussed in [**?**]. An uncorrelated systematic uncertainty of 3% is set as a function of centrality while a correlated one of 3% is set as a function of y. The extrapolated $\sigma^{pp}_{\Upsilon(1S)}$ cross section is reported with a fully correlated systematic uncertainty of 9% as a fonction of centrality and a fluctuation of 8-12% is given as a function of y. Finally, a fully correlated systematic uncertainty of 1% has been determined as a function of centrality and y. The procedure is describe in the Section 4 of the J/ψ analysis note (here) referring to the same Pb-Pb data sample (LHC15o period).

sources	Centrality		y	
	value (%)	type	value (%)	type
Input MC	1	I	1-3	II
Signal extraction	4-6	II	4-7	II
Tracker	3 and 0-1	I and II	1 and 3	I and II
Trigger	2	I	2	II
Matching	1	I	1	II
Centrality	0-5	II	0	I
F_{norm}	1	I	1	I
$\langle T_{\mathrm{AA}} \rangle$	3	II	3	I
$\sigma^{\mathrm{pp}}_{\Upsilon(1\mathrm{S})}$	9	I	8-12	II

Table 7: Summary of the systematic uncertainties. Type I (II) refers to a correlated (uncorrelated) systematic.

6 Results

Using all the ingredients describe above we are able to compute the $\Upsilon(1S)$ R_{AA}as a function of the collision centrality and the rapidity. The results are shown on the figure 13 and compared to the previous ALICE results obtained at lower energy. The ratio of ALICE results 5 TeV / 2.76 TeV is shown on the figure 14. The large uncertainties leads to a ratio compatible with unity nevertheless we observe a systematic increase of the R_{AA}. Finally, the results are compared to theoretical predictions (transport model) on the figure 15 and 16. The R_{AA}values are reported in the table 8 and 9.

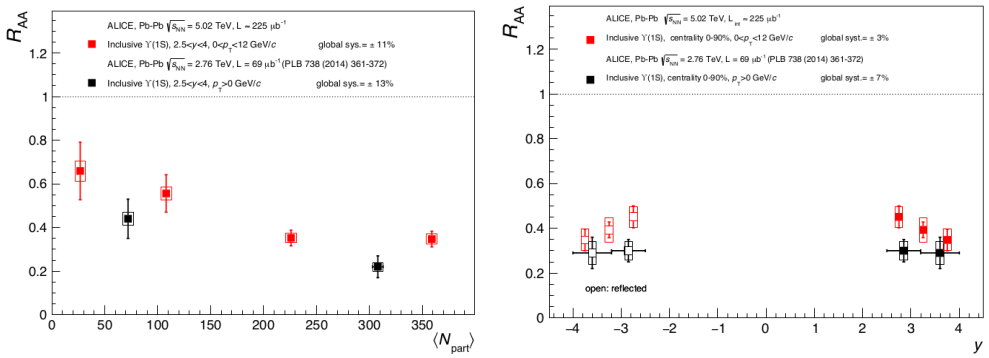

Fig. 13: R_{AA} vs centrality

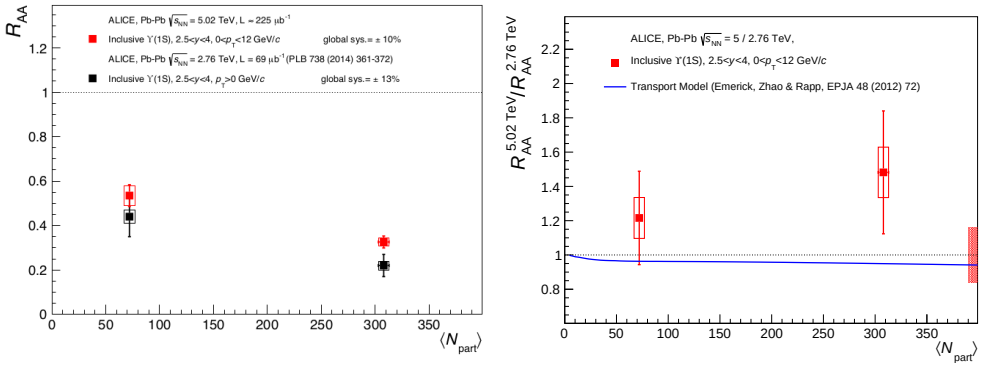

Fig. 14: R_{AA} vs centrality

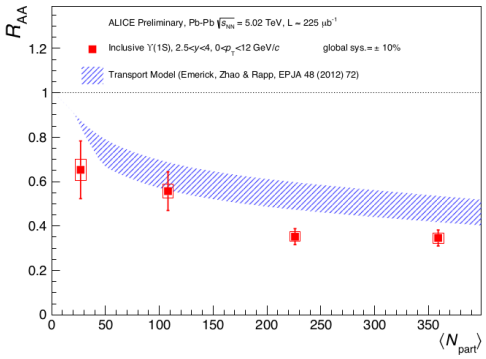

Fig. 15: R_{AA} vs centrality, Rapp & al model

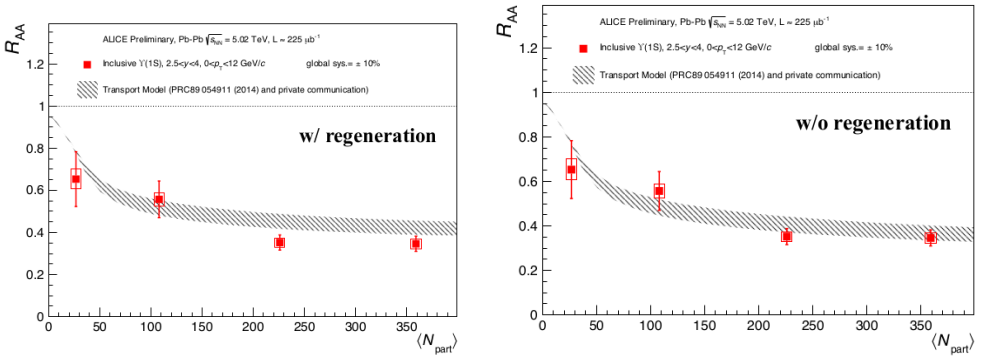

Fig. 16: $R_{\rm AA}$ vs centrality, Kai & al model

centrality	$R_{\rm AA}$ (Antoine)	$R_{\rm AA}$ (Indra)
$[0-10]\%$	$0.35 \pm 0.04(10.43\%) \pm 0.02(6.52\%) \pm 0.03(9.60\%)$	$0.36 \pm 0.04(12.01\%) \pm 0.03(7.63\%) \pm 0.03(9.60\%)$
$[10-30]\%$	$0.35 \pm 0.04(10.32\%) \pm 0.02(6.05\%) \pm 0.03(9.60\%)$	$0.32 \pm 0.04(11.38\%) \pm 0.04(11.29\%) \pm 0.03(9.60\%)$
$[30-50]\%$	$0.56 \pm 0.09(15.60\%) \pm 0.03(5.74\%) \pm 0.05(9.60\%)$	$0.51 \pm 0.07(14.00\%) \pm 0.05(10.11\%) \pm 0.05(9.60\%)$
$[50-90]\%$	$0.65 \pm 0.13(20.00\%) \pm 0.05(6.66\%) \pm 0.06(9.60\%)$	$0.65 \pm 0.13(20.00\%) \pm 0.06(9.61\%) \pm 0.06(9.60\%)$

Table 8: Centrality dependence of $\Upsilon(1S)$ $R_{\rm AA}$ at 5.02 TeV

rapidity	$R_{\rm AA}$ (Antoine)	$R_{\rm AA}$ (Indra)
$[2.5-3.0]$	$0.45 \pm 0.05(10.80\%) \pm 0.05(10.14\%) \pm 0.01(3.25\%)$	$0.38 \pm 0.05(12.43\%) \pm 0.05(12.58\%) \pm 0.01(3.25\%)$
$[3.0-3.5]$	$0.40 \pm 0.03(8.76\%) \pm 0.05(13.72\%) \pm 0.01(3.25\%)$	$0.38 \pm 0.04(10.00\%) \pm 0.05(13.15\%) \pm 0.01(3.25\%)$
$[3.5-4.0]$	$0.45 \pm 0.05(10.80\%) \pm 0.05(10.14\%) \pm 0.01(3.25\%)$	$0.30 \pm 0.05(15.13\%) \pm 0.04(12.69\%) \pm 0.01(3.25\%)$

Table 9: Rapidity dependence of $\Upsilon(1S)$ $R_{\rm AA}$ at 5.02 TeV

References

[1] Betty Bezverkhny Abelev et al. Suppression of $\Upsilon(1S)$ at forward rapidity in Pb-Pb collisions at $\sqrt{s_{\rm NN}} = 2.76$ TeV. *Phys. Lett.*, B738:361–372, 2014. *Cited page 2*

[2] Jaroslav Adam et al. Differential studies of inclusive J/ψ and ψ(2S) production at forward rapidity in Pb-Pb collisions at $\sqrt{s_{\rm NN}} = 2.76$ TeV. *JHEP*, 05:179, 2016. *Cited page 2*

[3] L. Aphecetche et al. Numerical simulations and offline reconstruction of the muon spectrometer of ALICE. ALICE Internal Note ALICE-INT-2009-044. *Cited page 2*

[4] The ALICE Collaboration. The ALICE experiment at the CERN LHC. *Journal of Instrumentation*, 3(08):S08002, 2008. *Cited page 2*